Bioorganic & Medicinal Chemistry 25 (2017) 3171–3181

Contents lists available at ScienceDirect

Bioorganic & Medicinal Chemistry

journal homepage: www.elsevier.com/locate/bmc

Synthesis, biochemical evaluation, and molecular modeling studies of aryl and arylalkyl di-*n*-butyl phosphates, effective butyrylcholinesterase inhibitors

Kensaku Nakayama [a,*], Jason P. Schwans [a,*], Eric J. Sorin [a,*], Trina Tran [a], Jeannette Gonzalez [a], Elvis Arteaga [a], Sean McCoy [a], Walter Alvarado [b]

[a] Department of Chemistry and Biochemistry, California State University, Long Beach, 1250 Bellflower Blvd., Long Beach, CA 90840, USA
[b] Department of Physics, California State University, Long Beach, 1250 Bellflower Blvd., Long Beach, CA 90840, USA

ARTICLE INFO

Article history:
Received 4 January 2017
Revised 29 March 2017
Accepted 3 April 2017
Available online 5 April 2017

Keywords:
Cholinesterase
Alzheimer's disease
Organophosphates
Enzyme inhibition
Computational docking

ABSTRACT

A series of dialkyl aryl phosphates and dialkyl arylalkyl phosphates were synthesized. Their inhibitory activities were evaluated against acetylcholinesterase (AChE) and butyrylcholinesterase (BChE). The di-*n*-butyl phosphate series consistently displayed selective inhibition of BChE over AChE. The most potent inhibitors of butyrylcholinesterase were di-*n*-butyl-3,5-dimethylphenyl phosphate (**4b**) [K_I = 1.0 ± 0.4 μM] and di-*n*-butyl 2-naphthyl phosphate (**5b**) [K_I = 1.9 ± 0.4 μM]. Molecular modeling was used to uncover three subsites within the active site gorge that accommodate the three substituents attached to the phosphate group. Phosphates **4b** and **5b** were found to bind to these three subsites in analogous fashion with the aromatic groups in both analogs being accommodated by the "lower region," while the lone pairs on the P═O oxygen atoms were oriented towards the oxyanion hole. In contrast, di-*n*-butyl-3,4-dimethylphenyl phosphate (**4a**) [K_I = 9 ± 1 μM], an isomer of **4b**, was found to orient its aromatic group in the "upper left region" subsite as placement of this group in the "lower region" resulted in significant steric hindrance by a ridge-like region in this subsite. Future studies will be designed to exploit these features in an effort to develop inhibitors of higher inhibitory strength against butyrylcholinesterase.

1. Introduction

Cholinesterase inhibitors are currently the major drug type in use to manage the progression of Alzheimer's disease (AD), the most common type of adult-onset dementia.[1] AD-associated cognitive impairment is correlated with acetylcholine (ACh) level reduction in the brain. This cognitive loss takes place in conjunction with changes in cholinesterase activity where acetylcholinesterase (AChE) activity decreases and butyrylcholinesterase (BChE) activity increases.[2] BChE activity in the AD brain is known to be elevated 40–65% above normal while AChE activity decreases to about 65% of the normal level.[2]

Since both AChE and BChE hydrolyze ACh, the use of cholinesterase inhibitors as treatment for AD is based on the hypothesis that the inhibition of these enzymes will increase the concentration of acetylcholine in the brain.[3] Thus, current treatment for AD involves the administration of reversible dual cholinesterase inhibitors, such as galantamine and tacrine, to suppress the activity of both AChE and BChE.[4] Recently, increased efforts are being made to develop cholinesterase inhibitors that target BChE in order to treat AD at more advanced stages.[5,6]

For example, cymserine analogs that selectively inhibited BChE were shown to raise ACh levels, improve cognition and lower β-amyloid peptide in rodent.[7] In addition, N1-phenethylnorcymserine, a BChE-selective inhibitor, suppressed cognitive dysfunction in mice challenged by amyloid-β peptide.[8] These results suggest that abnormal BChE activity increases the severity of cognitive dysfunction associated with AD. Therefore, it is possible that suitable BChE-inhibitors may have a significant role to play in the treatment of cognitive loss associated with AD.

The inhibition of the cholinesterases by organophosphorus insecticides and nerve toxins is widely appreciated.[9–11] Investigations into the selective inhibition of BChE over AChE by organophosphorus compounds is also receiving increased attention recently. For example, the exploration of organophosphates as AD therapeutics that are BChE-selective have been recently

* Corresponding authors.
E-mail addresses: Kensaku.nakayama@csulb.edu (K. Nakayama), Jason.schwans@csulb.edu (J.P. Schwans), Eric.sorin@csulb.edu (E.J. Sorin).

http://dx.doi.org/10.1016/j.bmc.2017.04.002
0968-0896/

reported by Richardson and co-workers.[12] Meanwhile, Sultatos and co-workers have reported the higher reactivity of the organophosphate chlorpyrifos towards BChE over AChE.[13] More recently, Kaboudin and Emadi found that phosphorothioates were moderately more selective inhibitors of BChE over AChE.[14] A recent study by Vinsova and co-workers has established that salicyanilide diethyl phosphates are excellent inhibitors of both AChE and BChE, with a preference for the latter enzyme, surpassing in some cases the inhibitory activity of the currently approved AD medications rivastigmine and galantamine.[15]

Some time ago, we systematically studied the inhibitory properties of a small library of dialkyl phenyl phosphates (DAPPs; Fig. 1) against AChE and BChE,[16] a family of compounds that possess some structural similarities to metrifonate, a dual cholinesterase inhibitor that raised acetylcholine levels and cognitive ability in AD patients during clinical trials.[17] We expected that the DAPPs should act as reversible inhibitors since they lack a good leaving group. We found that phosphate **1a** displayed the weakest inhibition against BChE among the series, while it was shown to be the most efficient inhibitor of AChE. Meanwhile, compound **1d** was the best inhibitor of BChE, while displaying no inhibition against AChE. Encouraged by these findings, we decided to explore the effects on inhibition against the cholinesterases, with particular focus on BChE, when systematic changes were introduced into the aromatic portion of the overall scaffold. The results of these studies are described herein.

2. Results and discussion

2.1. Chemistry

We studied a library of phosphates comprised of aryl di-*n*-butyl phosphates (**3a**–**3c**, **4a**–**c**, **5a**, **5b**), benzyl di-*n*-butyl phosphate (**6a**), di-*n*-butyl methylphenylmethyl phosphates (**6a**–**6d**), and di-*n*-butyl phenylethyl phosphate (**7**) (Fig. 2). As mentioned earlier, the library of compounds examined in our previous work[16] did not probe the effects of changes in the phenyl portion of the inhibitor scaffold on enzyme inhibition. In this study, one main goal was to explore how the methyl group location on the aromatic ring affects inhibition. We also changed the size of the phenyl ring by substituting it with a naphthyl group. In addition, we incorporated a methylene group as well as an ethyl chain between the phenyl ring and the phosphate oxygen atom to study the effects of these changes on enzyme inhibition.

In addition to the library of dibutyl phosphates listed in Fig. 2, we also prepared two aryl diethyl phosphates **8** and **9** (Fig. 3) which allowed us to study the effects of shortened alkyl chains on inhibition. These phosphates were prepared in acceptable yields and purity (>95% by GC/MS) by allowing either diethyl chlorophosphate **10** or di-*n*-butyl chlorophosphate **11** to react with an excess of the appropriate alcohol, R'OH, in the presence of pyridine (Scheme 1). Typical reaction times were approximately 12 h, except for the case when 1-naphthol was employed as the nucleophile, which required three days. All compounds were smoothly purified via column chromatography to afford colorless or near colorless oils that gave satisfactory ^{1}H NMR, ^{13}C NMR and mass spectral data.

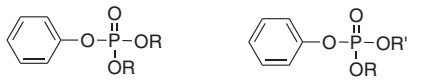

1a: R = CH_3
1b: R = CH_2CH_3
1c: R = $CH_2CH_2CH_3$
1d: R = $CH_2(CH_2)_2CH_3$
1e: R = $CH_2(CH_2)_3CH_3$
1f: R = *c*-C_6H_{11}

2: R = CH_2CH_2; R' = $CH_2(CH_2)_2CH_3$

Fig. 1. Library of dialkyl phenyl phosphates employed as inhibitors.

2.2. Enzyme inhibition studies

2.2.1. Evaluating the effect of adding substituents on the phenyl group of alkyl phenyl phosphates

As described above, Law et al. previously measured inhibition constants for a series of alkyl phenyl phosphates for BChE and AChE (Fig. 1).[16] Increasing the length of the alkyl groups from one to five carbons led to more potent inhibitors. Although comparison of the reported K_I values suggests the dipentyl phenyl phosphate was the most potent inhibitor relative to the shorter chain analogs (K_I = 6 μM (**1e**) versus K_I = 45–80 μM (**1c, 1d**), we recently observed that limited solubility affects the determination of the inhibition behavior of the dipentyl phenyl analog (unpublished results). The di-*n*-butyl phenyl analog, however, was soluble in the range of concentrations used to measure inhibition constants. We therefore investigated the effect of adding phenyl substituents in the di-*n*-butyl phenyl scaffold.

We first investigated the inhibitory behavior of introducing a methyl group on the phenyl ring at the 2-, 3-, or 4-position. The solubility of each analog in 2% methanol was evaluated using absorbance spectra. The absorbance increased linearly up to 0.5 mM suggesting the analogs are soluble at or below this concentration. To compare to prior results, we first measured the K_I value for dibutyl phenyl phosphate (**1d**) and obtained a K_I value of 100 μM, which is in agreement with previous studies. Butyrylcholinesterase from equine serum (E.C. Number 3.1.1.8) was used in all BChE inhibition studies. We then used the same approach to determine the K_I values for the phosphate analogs bearing methyl substituents on the phenyl ring (Table 1 and Fig. 4). Addition of dibutyl 2-methylphenyl phosphate (**3a**) led to a decrease in enzyme activity, but residual activity remained at the highest concentrations that could be tested. This could be due to the 2-methyl phenyl analog being a partial competitive inhibitor, or due to the inability to achieve concentrations high enough to abolish activity. Nevertheless, we can obtain a lower limit of 50 μM for the dibutyl 2-methylphenyl phosphate K_I value. In contrast, addition of dibutyl 3- and 4-methylphenyl phosphate reduced activity to levels indistinguishable from background suggesting that these analogs act as competitive inhibitors. The K_I values for dibutyl 3- and 4-methylphenyl phosphates (**3b** and **3c**) were 15 and 8 μM, respectively, indicating they are more potent inhibitors compared to the parental dibutyl phenyl phosphate (**1d**). To test if the analogs are selective inhibitors of BChE compared to other cholinesterases, we determined if the analogs inhibit AChE and/or chymotrypsin (Table 2). Previous studies have shown inhibition of each enzyme by organophosphates typically bearing smaller substituents than the compounds investigated herein. No significant inhibition of AChE was observed using inhibitor concentrations of 500 μM indicating the analogs are selective for BChE.

Prior studies reported organophosphate inhibitors of acetylcholinesterase are irreversible inhibitors in which the inhibitor covalently modifies the nucleophilic serine in the active site.[18,19] Alternatively, the compounds could interact with the active site through noncovalent interactions and bind reversibly. To test if compounds **3a**–**3c** act as irreversible or reversible inhibitors, we conducted substrate rescue experiments. Briefly, if the inhibitors covalently modify the active site (irreversible inhibition), then the addition of excess substrate is not expected to displace the compound and reverse inhibition. If the compounds are reversible inhibitors, then addition of excess substrate is expected to displace the inhibitor and rescue enzyme activity. As shown in Supplementary Content Table 1 addition of substrate rescued activity for com-

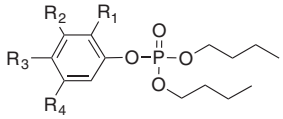

3a: $R_1 = CH_3$; $R_2 = R_3 = R_4 = H$
3b: $R_2 = CH_3$; $R_1 = R_3 = R_4 = H$
3c: $R_3 = CH_3$; $R_1 = R_2 = R_3 = H$
4a: $R_2 = R_3 = CH_3$; $R_1 = R_4 = H$
4b: $R_2 = R_4 = CH_3$; $R_1 = R_3 = H$
4c: $R_2 = R_3 = R_4 = CH_3$; $R_1 = H$

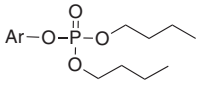

5a: Ar = 1-Naphthyl
5b: Ar = 2-Naphthyl

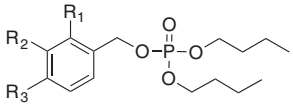

6a: $R_1 = R_2 = R_3 = R_4 = H$
6b: $R_1 = CH_3$; $R_2 = R_3 = H$
6c: $R_2 = CH_3$; $R_1 = R_3 = H$
6d: $R_3 = CH_3$; $R_1 = R_2 = H$

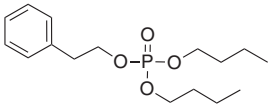

7

Fig. 2. Library of aryl/alkyl di-*n*-butyl phosphates studied in this work.

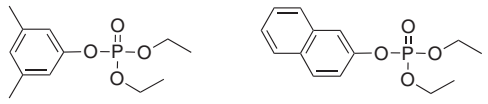

8 **9**

Fig. 3. Library of aryl diethyl phosphates studied in this work.

10: R = Et
11: R = *n*-Bu

3 - 9

Scheme 1. Synthesis of phosphates **3**–**9**. (i) Reagents: R′OH, pyridine, CH_2Cl_2, 0 °C–rt.

pounds **3a**–**3c**, suggesting the compounds act as reversible inhibitors. As a control, excess substrate did not rescue activity after incubation with the irreversible inhibitor dibutyl 2-chlorophenyl phosphate (**10** in Supplementary Content).

The K_I values for all methylphenyl analogs indicate that the methyl group on the phenyl ring leads to a better inhibitor compared to the phenyl group alone. The position of the methyl group is important as substitution at the 3- and 4-position led to 6–12-fold decrease in K_I, while substitution at the 2-position led to only a 2-fold effect. If a more potent inhibitor results from the addition of a methyl group that introduces favorable hydrophobic interactions with nonpolar groups in the active site, then the position of these hydrophobic interactions relative to the remainder of the phosphate inhibitor may be important. That is, each of the three analogs is expected to introduce the same increase in hydrophobicity compared to the unsubstituted case. However, substitution at the 3- or 4-position leads to a more potent inhibitor, relative to substitution at the 2-position, suggesting that unfavorable interactions are present when binding **3a** that is not found in **3b** or **3c**.

Building on the observation that methyl substitution at the 3- or 4-position of the phenyl ring leads to a better inhibitor compared to the phenyl group alone, we next tested di- and trimethyl analogs with methyl groups at the 3,4-, 3,5-, or 3,4,5-positions. If hydrophobic interactions with the individual methyl groups at the 3- and 4-position lead to a better inhibitor, then the introduction of methyl groups at multiple positions may further increase these interactions. The K_I values for 3,4-dimethyl phenyl phosphate (**4a**), 3,5-dimethyl phenyl phosphate (**4b**), and 3,4,5-trimethylphenyl phosphate (**4c**) are presented in Table 1. Results indicating the analogs are selective for BChE relative to AChE are presented in the Table 2. The K_I value for 3,5-dimethylphenyl phosphate, **4b**, was 95-fold lower than dibutyl phenyl phosphate **1d** and 15-fold lower than the analog bearing a single methyl group at the 3-position (**3b**) (Table 1). These results suggest that additional

Table 1
Potency of aryl/alkyl di-*n*-butyl.

No	R Group	K_I (μM)
3a		50 ± 16
3b		16 ± 2
3c		8 ± 1
4a		9 ± 1
4b		1.0 ± 0.4
4c		11 ± 1
5a		22 ± 2
5b	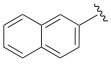	1.9 ± 0.4
6a		2 ± 1
6b		72 ± 2
6c		24 ± 8
6d	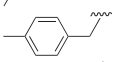	14 ± 6
7	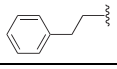	53 ± 1

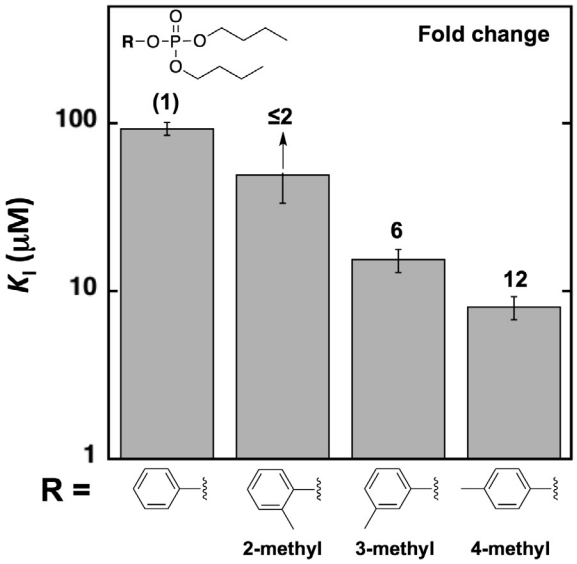

Fig. 4. Effects of methyl substituents on the K_I value. Values and errors are averages and SDs from three or more independent measurements and are from Table 1.

Table 2
Relative activity of AChE, BChE, and chymotrypsin.

Analog	BChE[a] Activity ratio*	AChE[b] Activity ratio*	Chymotrypsin[c] Activity ratio*
3a	0.27 ± 0.03	0.99 ± 0.01	0.92 ± 0.05
3b	0.15 ± 0.02	0.99 ± 0.07	0.89 ± 0.04
3c	0.02 ± 0.01	0.89 ± 0.01	0.96 ± 0.01
4a	0.04 ± 0.02	1.04 ± 0.04	0.94 ± 0.02
4b	0.01 ± 0.01	1.00 ± 0.08	0.95 ± 0.04
4c	0.09 ± 0.01	1.09 ± 0.02	0.84 ± 0.10
5a	0.21 ± 0.01	1.07 ± 0.01	0.93 ± 0.04
5b	0.01 ± 0.01	1.05 ± 0.07	0.76 ± 0.05
6a	0.01 ± 0.01	1.00 ± 0.01	0.97 ± 0.02
6b	0.04 ± 0.01	0.98 ± 0.07	0.94 ± 0.08
6c	0.12 ± 0.01	0.86 ± 0.01	0.94 ± 0.06
6d	0.04 ± 0.02	0.87 ± 0.05	0.92 ± 0.08
7	0.11 ± 0.01	1.02 ± 0.03	0.89 ± 0.02

* Activity ratio = 500 μM Inhibitor/No Inhibitor.
[a] BChE from equine serum (E.C. 3.1.1.8).
[b] AChE from *Electrophorus electricus* (E.C. 3.1.1.7).
[c] Chymotrypsin from bovine pancreas (E.C. 3.4.21.1).

favorable hydrophobic interactions are made with an analog bearing methyl groups at the two *meta* positions. Meanwhile, where addition of a methyl group at the 4-position led to a lower K_I value relative to the unsubstituted phenyl ring, addition of a 4-methyl group in an analog bearing methyl groups at the 3, 5-postions actually increased the K_I value by 10-fold. This suggests that simply increasing the steric bulk does not necessarily lead to an inhibitor with a lower K_I value. The context in which the steric bulk is added affects whether additional methyl groups lead to a better inhibitor.

2.2.2. Evaluating dialkyl benzyl analogs as BChE inhibitors

We next examined benzyl dialkyl phosphate analogs to test if introducing conformational flexibility of the aromatic group relative to the phosphate leads to better inhibitors. Inspection of BChE X-ray structures with ligands bearing aromatic groups bound show the aromatic groups situated in different conformations. While previous modeling studies have suggested conformations in which the dialkyl phenyl phosphates are bound, experimental data supporting these binding conformations are not available. The greater conformational flexibility of the benzyl versus phenyl group might allow the substituted aromatic group to adopt a conformation leading to more favorable hydrophobic interactions and thus increase binding.

We first measured the K_I value for benzyl dibutyl phosphate (**6a**) and compared the results to the dibutyl phenyl phosphate (**1d**) (Table 1 and Fig. 5). The K_I value of 2.3 μM was ~50-fold lower than the value for the corresponding phenyl analog. This suggests that the additional conformational flexibility afforded by the benzyl linker allows the phenyl group to adopt a conformation that leads to more favorable binding interactions or may permit the aromatic group to adopt a conformation that reduces unfavorable interactions.

If a single methylene group between the phosphate and aromatic ring results in a ~50-fold lower K_I value, then additional methylene groups that introduce even greater conformational flexibility may lead to the aromatic group being positioned to make more favorable binding interactions. To test this possibility, we determined the K_I value for phenethyl phosphate **7** (fig. 5). The 2-carbon linker analog displayed a K_I value of 53 μM, within 2-fold of dibutyl phenyl phosphate, and a 28-fold higher K_I value than that for **6a**. Inhibition of **6a**–**6d** was rescued by excess substrate suggesting the compounds are reversible inhibitors (Supplementary Content Table 1).

As described above, methyl substitutions on the aromatic ring lead to lower K_I values. To test if methyl substitutions on the aromatic ring lead to better inhibitors in the benzyl dibutyl scaffold, we measured the K_I values for dibutyl phosphates bearing a 2-, 3-, or 4-methyl benzyl group (**6b**–**6d**) (Fig. 5). In contrast to the results for the methylphenyl series, all methyl group substitutions on the benzyl scaffold led to poorer inhibitors relative to **6a**. This result suggests that simply introducing steric bulk to increase van der Waals interactions may not lead to better inhibitors.

2.2.3. Effect of expanding the aromatic moiety for dialkyl aryl phosphate inhibitors

A number of cholinesterase inhibitors, such as tacrine, rivastigmine and galantamine, bear aromatic groups. The X-ray crystallographic structures of BChE show the active site lined with aromatic and hydrophobic groups and inhibitors containing aromatic groups can make favorable binding interactions via van der Waals

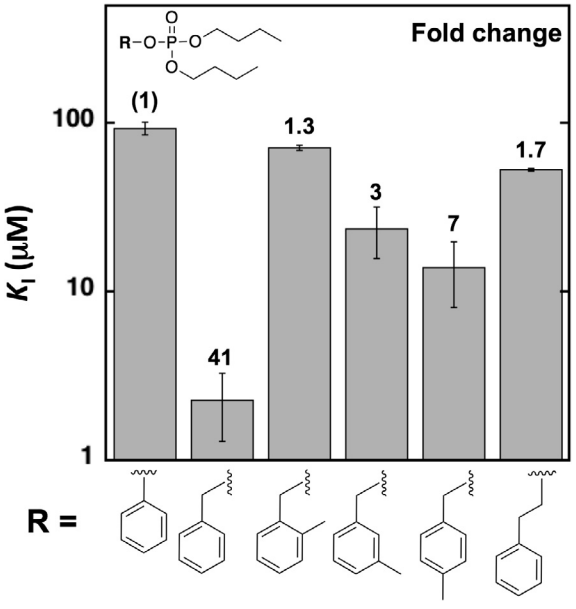

Fig. 5. Effects of methyl substitutions on K_I values in the benzyl scaffold. Values and errors are averages and SDs from three or more independent measurements and are from Table 1.

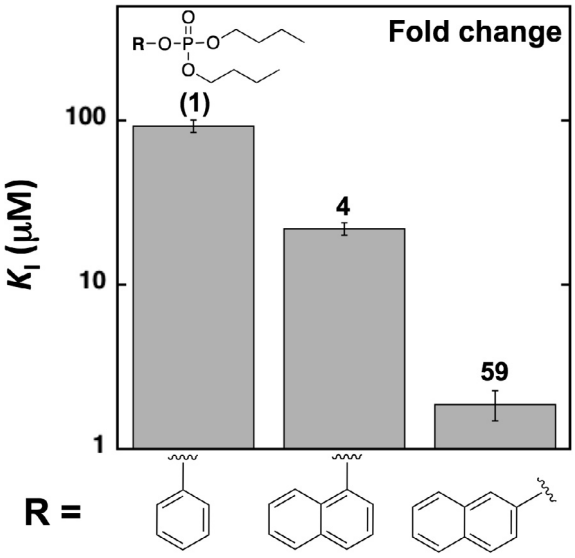

Fig. 6. Effects of naphthyl substitutions on K_I. Values and errors are averages and SDs from three or more independent measurements and are from Table 1.

interactions and/or pi-pi stacking. To test if expanding the aromatic moiety in a dialkyl phosphate leads to a more potent inhibitor, we examined the effect of introducing a 1- and 2-naphthyl group in the dibutyl phosphate scaffold. The K_I values of 22.2 and 1.9 μM for dibutyl 1-naphthyl phosphate (**5a**) and dibutyl 2-naphthyl phosphate (**5b**), respectively, were lower than the dibutyl phenyl analog suggesting that the larger aromatic moiety leads to more potent inhibitors (Table 1 and Fig. 6). Enzyme activity was rescued in the presence of excess substrate suggesting the compounds are reversible inhibitors (Supplementary Content Table 1). The ~10-fold difference in K_I values for the naphthyl analogs suggests that the position of the naphthyl group relative to the phosphate affects the inhibition properties. It is possible that this is related to the earlier observation that methyl group substitution at the 3- and 4-position of the phenyl group leads to more effective inhibitors compared to substitution of the 2-position. In the 2-naphthyl analog, the benzene ring is connected to another aromatic ring at the 3- and 4-position, whereas in the 1-naphthyl analog the benzene ring is connected to another ring at the 2- and 3-positon. For the phenyl analogs described above methyl substitution at the 3- and 4-position lead to inhibitors with significantly lower K_I values than the phenyl analog substituted at the 2-position. This suggests that alkyl or aromatic substitutions at the 2-position prevents the alkyl or aromatic group from making favorable interactions, or substitution at the position closest to the phosphate leads to unfavorable interactions leading to weaker binding.

2.2.4. Using dialkyl aryl phosphates to probe the connection of groups within inhibitors and inhibition behavior

The idiosyncratic composition of enzyme active sites introduces many challenges in the design of effective inhibitors. While a series of molecules with varying substituents at a position can be screened to identify candidate inhibitors, these changes can affect the contribution to binding for other groups in the inhibitor. Phosphates **3**–**7** offered a convenient system in which to explore the connection between different groups on the inhibitor and the inhibition behavior, as changes can be readily introduced on the phenyl ring and the alkyl chains can be varied to probe the connection between the different groups and the inhibition properties.

To further probe this connection we investigated the effect of perturbing the dialkyl chains using the two inhibitors that showed the lowest K_I values in the results described above: 3,5-dimethyl phenyl and 2-naphthyl analogs (**4b** and **5b**). As previously noted, Law et al. reported that increasing the length of the dialkyl groups lead to inhibitors with lower K_I values and inhibitors more selective for BChE relative to AChE. To evaluate the connection between the length of the alkyl chain and the identity of the aromatic group, we compared the inhibition properties of aryl diethyl phosphates **8** and **9** and aryl di-*n*-butyl phosphates **4b** and **5b**, which bear either 3,5-dimethylphenyl or 2-naphthyl groups.

In the diethyl phosphate scaffold, introduction of the 3,5-dimethyl groups led to a 3-fold decrease in the K_I value (Table 3 and Fig. 7), and is significantly less than the 94-fold lower K_I value determined for introducing the 3,5-dimethylgroups in the dibutyl scaffold. Similarly, expanding the aryl system from phenyl to 2-naphthyl led to smaller lowering in K_I value in the diethyl relative to the dibutyl analog, 11-fold compared to 50-fold, respectively. Our results suggest that contribution of the aromatic moiety to inhibition is affected by the identity of the alkyl chains as well. The presence of the longer dialkyl chains could affect the position of the ligand bound in the active site allowing more extensive van der Waals interactions in the dibutyl analogs leading to lower K_I values.

3. Molecular modeling studies

In discussing our molecular modeling results, we focus on the following three subgroups of inhibitors examined in this study: the di-*n*-butyl methylphenyl series; the di-*n*-butyl naphthyl series; and the di-*n*-butyl dimethylphenyl and trimethylphenyl series (Fig. 8).

Our massive docking trials for each of the inhibitors in these three subgroups have led to two primary observations regarding possible binding modes for these species. First and foremost, the aromatic-group bearing substituent, ArO-, may be located in one of two possible regions within the active site pocket, the first of which will be defined as the "lower region" of the pocket, near residues Y128 and Q67, and bounded by residues T120 and choline-binding W82. This first orientation is that assumed by the control species, dibutyl phenyl phosphate (**1d**). The alternative ArO-group position, near W430 and Y440, will be defined as the "upper left region" of the pocket. Fig. 9a–c provide identical views of bound inhibitors of the methylphenyl series from the perspective of one looking directly into the binding pocket from the external opening of the active site gorge and illustrate these two regions clearly. The preference of a given ArO-group for one or both of these regions is dependent on the steric factors and the chemistry of these regions and of the respective inhibitor under consideration.

As a result of ArO-group positioning, the P═O oxygen can take on multiple orientations with respect to the binding pocket. In one possible orientation, this oxygen points "out of pocket" toward

Table 3
Potency of aryl di-*n*-ethyl phosphates.

No	R Group	K_I (μM)
–[a]		1590 ± 40
8		583 ± 61
9	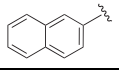	147 ± 10

[a] Synthesis of di-*n*-ethyl phenyl phosphate reported in Law et al.

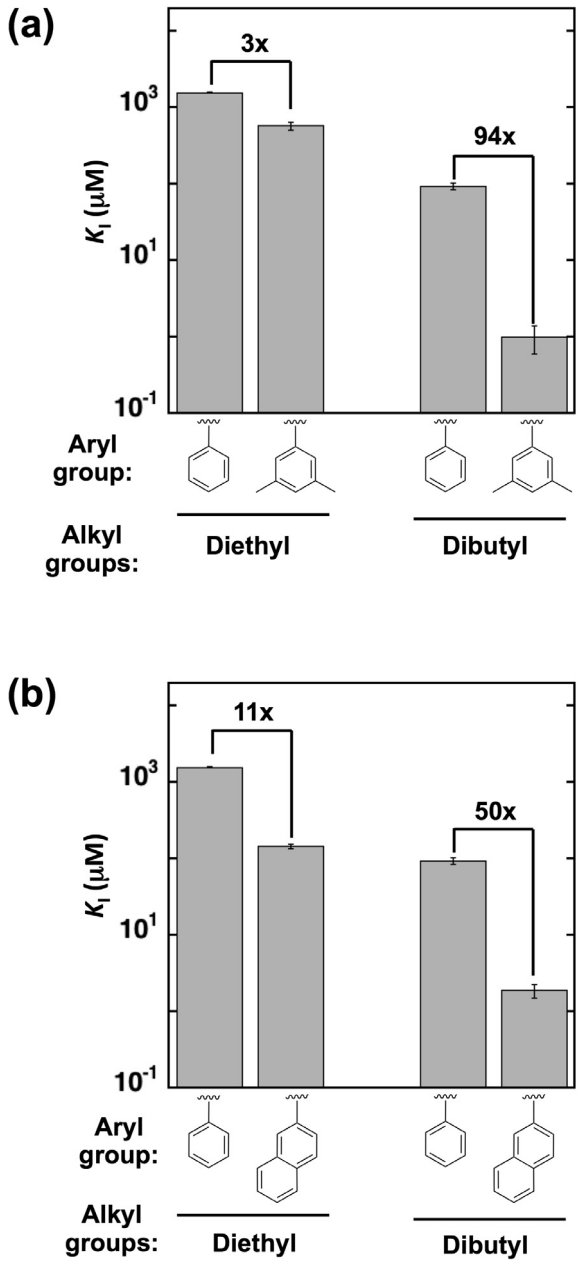

Fig. 7. Testing the effect of aromatic substitutions in diethyl and dibutyl phosphate scaffolds. Effects of the 3,5-dimethyl (A) and 2-naphthyl (B) substitutions on the K_I value in the diethyl and dibutyl phosphate scaffolds. Values and errors are averages and SDs from three or more independent measurements and are from Tables 1 and 3.

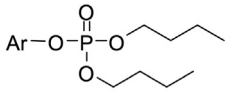

Ar = 2-methylphenyl; 3-methylphenyl;
4-methylphenyl; 1-naphthyl; 2-naphthyl;
3,4-dimethylphenyl; 3,5-dimethyllphenyl;
3,4,5-trimethylphenyl

Fig. 8. Inhibitors discussed in this subsection.

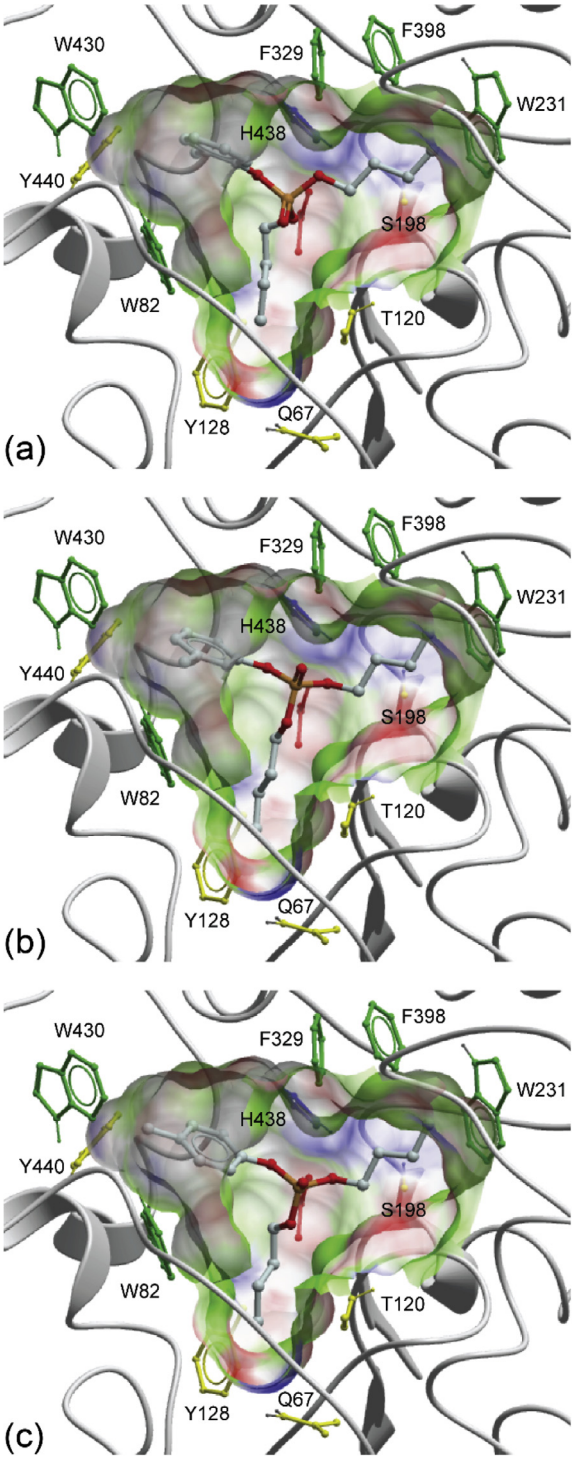

Fig. 9. Binding poses of the (a) *o*-methylphenyl (**3a**), (b) *m*-methylphenyl (**3b**), and (c) *p*-methylphenyl dibutyl phosphate (**3c**) inhibitors in the active site of BChE from the perspective of one viewing from the external entrance of the binding site gorge. The pocket surface is color-coded to distinguish neutral (white), hydrophobic (green), anionic/hydrogen bond acceptor (red), and cationic/hydrogen bond donor (blue) regions. Secondary structure of the surrounding region is shown as white ribbons to convey the relative orientation of the protein.

the external opening of the gorge, fully solvent-exposed and lacking interactions with residues within the gorge. Alternatively, this oxygen can point "into pocket" and take on one of two notable orientations. When this oxygen takes on a downward facing orientation, strong interactions with hydrogen bonding partners in the oxyanion hole (G116, G117, and A199) are present. When this oxygen instead assumes an upward or rear-facing orientation, hydrogen bonding with these residues is less significant, or lost entirely,

and an unfavorable interaction with the carboxyl group of residue E197 in the rear of the pocket occurs, making the former orientation the preferred of the three orientations observed and the latter the least favorable.

As illustrated in Fig. 9a–c, the di-*n*-butyl methylphenyl series **3a**–**3c** prefer ArO-group placement in the upper left region of the pocket with the P═O oxygen pointing "out of pocket" and thus leaving this moiety largely unimportant in the binding energetics of these species. Observed docking scores reproduced the experimentally observed inhibition trend, with the *p*-methylphenyl analog binding favored over the *m*-methylphenyl, and the *m*-methylphenyl analog binding favored over *o*-methyl. Structural analysis shows that the *o*-methylphenyl substituent (**3a**) takes on a rear-facing orientation (Fig. 9a), located in a vacant region of the pocket relatively void of potential interaction partners, and rotation of the *o*-methylphenyl group by ~180° would lead to considerable steric clash with the phosphate group. This lack of significant participation by the methyl substituent during binding results in this species having relatively weak inhibitory power, on the order of that of the control species, dibutyl phenyl phosphate (**1d**). In comparison, the *m*-methyl substituent (**3b**) prefers a forward facing orientation while avoiding the previously mentioned steric clash with the inhibitor phosphate group (Fig. 9b). This orientation allows *m*-methyl interaction with the sidechain of W430, thereby stabilizing the binding of this species. Of the three possible substituent placements, this interaction is maximized by the *p*-methyl species (**3c**), resulting in further enhancement of binding strength and inhibitory power (Fig. 9c).

The preferred binding modes of the 1-naphthyl (**5a**) and 2-naphthyl (**5b**) substituted species are shown in Fig. 10a and b, respectively, with lower panels presenting the same poses as viewed after rotation of 80° about the vertical axis. The lower region of the pocket provides ample volume for the placement of the naphthyl group substituents. In both cases, ArO-group interaction with the choline-binding W82 residue is apparent and the P═O oxygen is oriented "into pocket." Yet, subtle but important differences are also observed, leading to the 2-naphthyl species being a significantly more effective inhibitor, again in agreement with our experimental observations. The lower panels of Fig. 10 illustrate the contrast in positioning of the 1-naphthyl (**5a**) and 2-naphthyl (**5b**) ArO-groups, with the former being positioned farther inside the binding pocket and thus more sterically confined than the latter species. This positioning of the 1-naphthyl species leaves the P═O oxygen positioned in significant contact with the E197 carboxyl group, while also limiting interactions with hydrogen bonding partners in the oxyanion hole (G116, G117, and A199). In addition, the 1-naphthyl species has only limited interaction with the hydroxyl group of T120 and cannot interact with residue Q67. In contrast, the location of the 2-naphthyl substituent allows significant interactions with both the entire T120 sidechain and the amine group of Q67, thereby providing numerous interactions by which this inhibitor is stabilized.

Following our observations that larger ArO-groups can be sterically limited to the lower region of the pocket, and that the location of a methyl substituent on the phenyl group can enhance inhibitory activity to varying degrees, we assessed the experimentally observed trends among di-*n*-butyl dimethylphenyl and trimethylphenyl phosphates **4a**–**4c**. Of the three species studied, a structural trend was quickly identified – though larger than their monomethyl analogs, the 3,4-dimethylphenyl (**4a**) and 3,4,5-trimethylphenyl (**4c**) ArO-groups are unable to occupy the lower region of the pocket, as do the naphthyl groups: the *p*-methyl substituent present in these species conflicting with a structural "ridge" present at the bottom of the pocket between residues Y128 and Q67. Fig. 11a illustrates the resulting pose of the 3,4-dimethylphenyl species, with the ArO-group located in the upper left region of the pocket. This species assumes the same docking pose as that of the *para* monomethyl species (**3c**), with an added methyl group in the *meta* position on the phenyl ring. Yet this added *m*-methyl group adds no significant interactions with

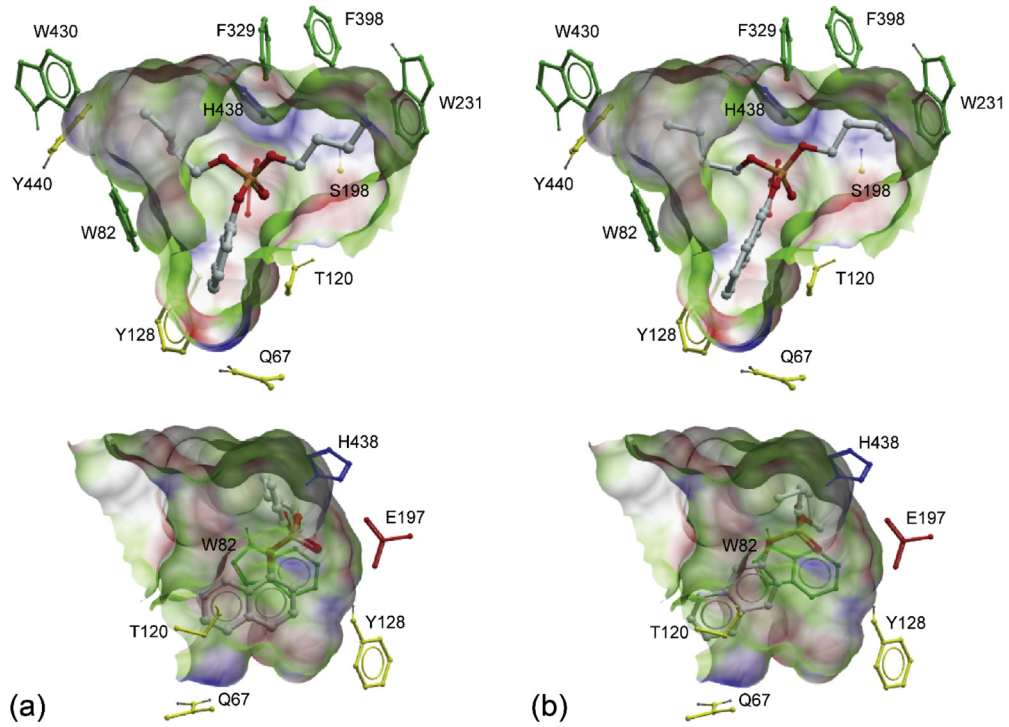

Fig. 10. Binding poses of the (a) 1-napthyl and (b) 2-naphtyl dibutyl phosphate inhibitors in the BChE active site, with color coding following that of Fig. 9. Top panel images are oriented identically to Fig. 9 images, with bottom panels rotated 80° around the vertical axis. Secondary structure of the surrounding region is omitted to best illustrate protein-inhibitor interactions.

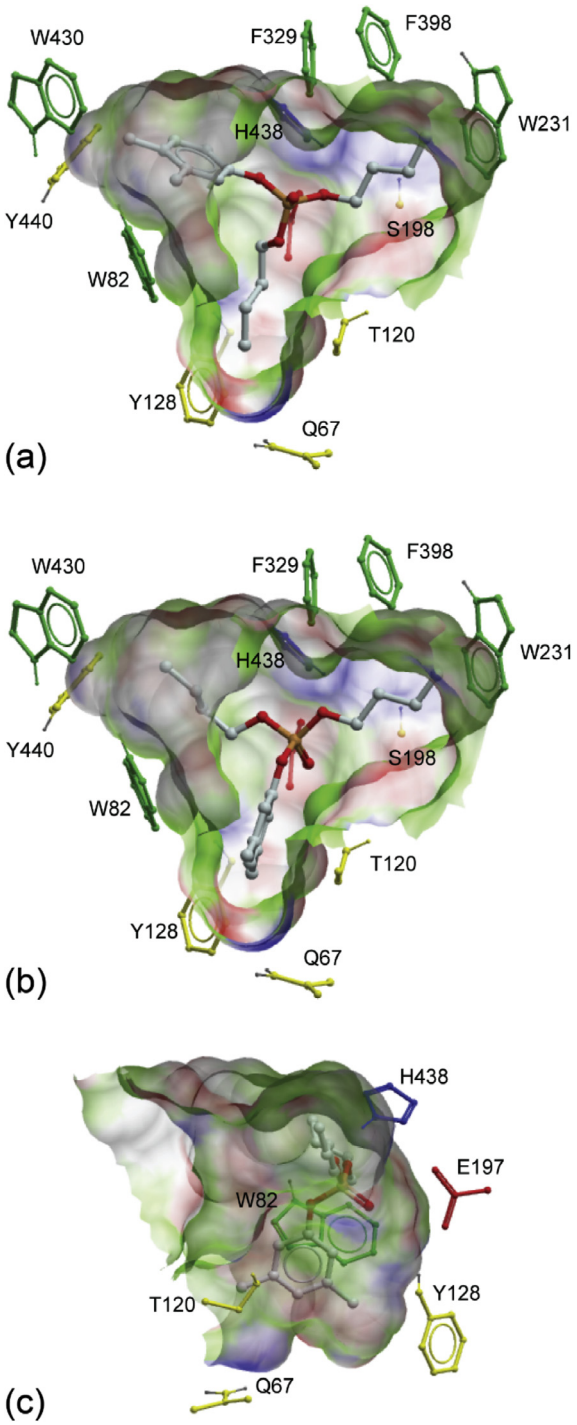

Fig. 11. Binding poses of the (a) 3,4-dimethylphenyl and (b) 3,5-dimethylphenyl dibutyl phosphate inhibitors in the BChE active site oriented identically to that in Fig. 9. (c) Binding pose of the 3,5-dimethylphenyl species shown in (b) rotated 80° around the vertical axis. Color coding follows that of Fig. 9 and secondary structure of the surrounding region is omitted to best illustrate protein-inhibitor interactions.

pocket residues, resulting in nearly identical inhibitory power as that of di-*n*-butyl *p*-methylphenyl phosphate (**3c**).

In striking contrast, the 3,5-dimethylphenyl substituent of **4b**, with a more broad ArO-group profile, does not suffer the *p*-methylphenyl steric clash in the lower region of the pocket described above, and this ArO-group is thus located in that lower region (Fig. 11b). This orientation allows the P═O oxygen to point "into pocket" in a downward facing direction, thereby fostering interactions with hydrogen bonding partners in the oxyanion hole that are lacking in the "out of pocket" oxygen orientation of the 3,4-dimethyl species (**4a**). Similar to the observed docking poses of the 1-naphthyl (**5a**) and 2-naphthyl species (**5b**), placement of the ArO-group in the lower region of the pocket (Fig. 11c) allows significant interaction between the 3,5-dimethyl groups and both W82 and T120. Additional interactions between the two *m*-methyl groups and residues Q67 and Y128 provide added binding strength, thereby giving this species inhibitory power on par with the highly-effective 2-naphthyl species (**5b**).

Lastly, unlike the 3,5-dimethyl species (**4b**), the *p*-methyl substituent on the 3,4,5-trimethylphenyl moiety (**4c**) causes the ArO-group to again be located in the upper left region of the pocket (pose not shown), as in the case of di-*n*-butyl *p*-methylphenyl phosphate (**3c**). The added *m*-methyl substituent results in a slight rotation of the ArO-group, similar to that observed for the *o*-methyl species (**3a**) and positions the added *m*-methyl group in the vacant region toward the rear of the pocket, as described above for **3a** (Fig. 9a). No significant interactions to affect binding strength result from this added methyl substituent, leaving this species nearly equal in inhibitory power as di-*n*-butyl 3,4-dimethylphenyl phosphate (**4a**) and di-*n*-butyl *p*-methylphenyl phosphate (**3c**).

4. Conclusions

By studying the effects of introducing relatively simple changes in the structure of the original phosphate **1d** on BChE inhibition, we were able to develop several very potent, highly selective BChE inhibitors with K_I values down to 1/95th that of phosphate **1d**. Our computational studies uncovered two major binding modes for this class of inhibitors, where the substituent bearing the aromatic group could occupy either the "upper left region" or the "lower region" of the three subsites in the BChE active site gorge. Phosphates **4b** and **5b**, two of the most effective inhibitors, both preferred to place their aromatic groups in the "lower region", which also allowed the P═O moiety to interact with hydrogen bond donor groups in the oxyanion hole.

This study demonstrates the utility of employing P(V) triesters as possible transition state or tetrahedral intermediate mimics in developing effective inhibitors for the cholinesterases. While clinically important cholinesterase inhibitors generally have K_I values in the nanomolar range and the current inhibitors show K_I values in the micromolar range, the ease and flexibility by which structural variations can be introduced into these triesters magnifies their utility as a scaffold for new inhibitors. We are currently studying ways to exploit these findings to design new inhibitors possessing even greater inhibitory properties.

5. Experimental section

5.1. Chemistry

Diethyl chlorophosphate, di-*n*-butyl chlorophosphate and the alcohols were used as received from commercial suppliers without further purification. Methylene chloride (DCM) and pyridine were dried and stored over 3 Å molecular sieves. All glassware was dried and purged with dry nitrogen before use. All reactions were performed under dry nitrogen. The rotary evaporator used was Buchi R-3. Flash chromatographic purifications were performed by using silica gel (flash-grade) from Dynamic Adsorbents Inc. and hexane and ethyl acetate as solvent system. TLCs were ran on Whatman glass-backed silica gel plates and visualized with UV light and phosphomolybdic acid (10%) in ethanol solution. NMR spectra were obtained on either a Bruker Fourier 300 MHz or Bruker Avance III 400 MHz spectrometer with $CDCl_3$ as the solvent and

$CHCl_3$ residual peak as reference. Chemical shifts are given in parts per million (ppm), and all coupling constants (*J*) are given in hertz (Hz). GC/MS analyses were performed on an Agilent 7820A/5975 GC/MS instrument. High resolution mass spectra (HRMS) were obtained by the UCR Mass Spectrometry Facility on an Agilent 6210 LCTOF instrument operated in the multimode source configuration.

5.1.1. General procedure for the preparation of triphosphates

To a dried two or three-necked 150 mL round bottom flask, 1.04 mL (1.14 g, 5.00 mmol) of di-*n*-butyl chlorophosphate was dissolved in 12 mL CH_2Cl_2 with stirring. The solution was cooled to 0 °C. Then 2.0 equivalents of alcohol and 2.0 equivalents of pyridine were added to the solution via syringe. The reaction was stirred overnight at room temperature. The reaction mixture was diluted with 80 mL of diethyl ether and washed three times with 30 mL of 10% HCl. The aqueous layers were combined and washed with 40 mL of CH_2Cl_2. The combined organic layer was washed once with 40 mL of saturated sodium bicarbonate, once with 40 mL of brine, dried over magnesium sulfate, filtered, concentrated *in vacuo*. The products were purified by flash chromatography.

*5.1.1.1. Di-n-butyl phenyl phosphate (**1d**).* Following the general procedure described above and using phenol, **1d** was obtained as a yellow oil: 50% yield. ^{1}H NMR (300 MHz, $CDCl_3$) δ 0.91 (t, J = 7.8 Hz, 6H, ($OCH_2CH_2CH_2CH_3)_2$), 1.33–1.45 (m, 4H, ($OCH_2CH_2CH_2CH_3)_2$), 1.62–1.71 (m, 4H, ($OCH_2CH_2CH_2CH_3)_2$), 4.06–4.19 (m, 4H, ($OCH_2CH_2CH_2CH_3)_2$), 7.13–7.35 (m, 5H, Ph-*H*); ^{13}C NMR (75 MHz, $CDCl_3$) δ 13.52, 18.60, 32.24, 68.32, 119.93, 124.94, 129.67, 150.74. MS (gc/ms) *m*/*z* (%): 286 (M^+, 8.4), 175 (100), 94 (54.9).

*5.1.1.2. Di-n-butyl o-methylphenyl phosphate (**3a**).* Following the general procedure described above and using *o*-methylphenol, **3a** was obtained as a light yellow oil: 37% yield. ^{1}H NMR (300 MHz, $CDCl_3$) δ 0.91 (t, J = 7.4 Hz, 6H, ($OCH_2CH_2CH_2CH_3)_2$), 1.33–1.45 (m, 4H, ($OCH_2CH_2CH_2CH_3)_2$), 1.62–1.71 (m, 4H, ($OCH_2CH_2CH_2CH_3)_2$), 2.31 (s, 3H, Ph-CH_3), 4.09–4.19 (m, 4H, ($OCH_2CH_2CH_2CH_3)_2$), 7.03–7.29 (m, 4H, Ar-*H*); ^{13}C NMR (75 MHz, $CDCl_3$) δ 15.53, 16.34, 18.62, 32.19, 68.26, 119.70, 124.86, 126.96, 129.25, 131.26,149.22. MS (gc/ms) *m*/*z* (%): 300 (M^+, 45.9), 188 (100), 107 (100). HRMS: *m*/*z* calculated for $C_{15}H_{26}O_4P$ (MH^+) 301.1563. Found 301.1521.

*5.1.1.3. Di-n-butyl m-methylphenyl phosphate (**3b**).* Following the general procedure described above and using *m*-methylphenol, **3b** was obtained as a light yellow oil: 39% yield. ^{1}H NMR (300 MHz, $CDCl_3$) δ 0.84 (t, J = 7.4 Hz, 6H, ($OCH_2CH_2CH_2CH_3)_2$), 1.26–1.38 (m, 4H, ($OCH_2CH_2CH_2CH_3)_2$), 1.55–1.64 (m, 4H, ($OCH_2CH_2CH_2CH_3)_2$), 2.26 (s, 3H, Ph-CH_3), 4.03–4.10 (m, 4H, ($OCH_2CH_2CH_2CH_3)_2$), 6.88–7.21 (m, 4H, Ar-*H*); ^{13}C NMR (75 MHz, $CDCl_3$) δ 13.53, 18.61, 21.30, 32.16, 68.22, 116.84, 120.59, 125.67, 129.31, 139.86,150.67. MS (gc/ms) *m*/*z* (%): 300 (M^+, 43.7), 188 (100), 108 (49.2). HRMS: *m*/*z* calculated for $C_{15}H_{26}O_4P$ (MH^+) 301.1563. Found 301.1531.

*5.1.1.4. Di-n-butyl p-methylphenyl phosphate (**3c**).* Following the general procedure described above and using *p*-methylphenol, **3c** was obtained as a colorless oil: 40% yield. ^{1}H NMR (300 MHz, $CDCl_3$) δ 0.92 (t, J = 7.4 Hz, 6H, ($OCH_2CH_2CH_2CH_3)_2$), 1.33–1.46 (m, 4H, ($OCH_2CH_2CH_2CH_3)_2$), 1.62–1.71 (m, 4H, ($OCH_2CH_2CH_2CH_3)_2$), 2.31 (s, 3H, Ph-CH_3), 4.09–4.18 (m, 4H, ($OCH_2CH_2CH_2CH_3)_2$), 7.07–7.14 (m, 4H, Ar-*H*); ^{13}C NMR (75 MHz, $CDCl_3$) δ 13.54, 18.62, 20.71, 32.17, 68.14, 119.71, 130.10, 134.48, 148.64. MS (gc/ms) *m*/*z* (%): 300 (M^+, 38.6), 188 (100), 108 (76.8). HRMS: *m*/*z* calculated for $C_{15}H_{26}O_4P$ (MH^+) 301.1563. Found 301.1528.

*5.1.1.5. Di-n-butyl 3, 4-dimethylphenyl phosphate (**4a**).* Following the general procedure described above and using 3, 4-dimethylphenol, **4a** was obtained as a light yellow oil: 39% yield. ^{1}H NMR (300 MHz, $CDCl_3$) δ 0.92 (t, J = 7.4 Hz, 6H, ($OCH_2CH_2CH_2CH_3)_2$), 1.34–1.46 (m, 4H, ($OCH_2CH_2CH_2CH_3)_2$), 1.62–1.71 (m, 4H, ($OCH_2CH_2CH_2CH_3)_2$), 2.21 (s, 3H, Ph-CH_3), 2.23 (s, 3H, Ph-CH_3), 4.09–4.16 (m, 4H, ($OCH_2CH_2CH_2CH_3)_2$), 6.92–7.07 (m, 3H, Ar-*H*); ^{13}C NMR (75 MHz, $CDCl_3$) δ 14.12, 19.18, 20.45, 3.1.51, 68.63, 69.01, 117.49, 121.46, 130.96, 133.68, 138.65, 149.17. MS (GC/MS) *m*/*z* (%): 314 (M^+, 71), 258 (71), 203 (100). HRMS: *m*/*z* calculated for $C_{16}H_{28}O_4P$ (MH^+) 315.1720. Found 315.1663.

*5.1.1.6. Di-n-butyl 3, 5-dimethylphenyl phosphate (**4b**).* Following the general procedure described above and using 3, 5-dimethylphenol, **4b** was obtained as a yellow oil: 43% yield. ^{1}H NMR (400 MHz, $CDCl_3$) δ 0.89 (t, J = 7.4 Hz, 6H, ($OCH_2CH_2CH_2CH_3)_2$), 1.33–1.42 (m, 4H, ($OCH_2CH_2CH_2CH_3)_2$), 1.61–1.68 (m, 4H, ($OCH_2CH_2CH_2CH_3)_2$), 2.26 (s, 6H, Ph-($CH_3)_2$), 4.08–4.13 (m, 4H, ($OCH_2CH_2CH_2CH_3)_2$), 6.76 (s, 1H, Ar-*H*), 6.81 (s, 2H, Ar-*H*); ^{13}C NMR (100 MHz, $CDCl_3$) δ 11.66, 16.79, 19.35, 30.43, 66.31, 115.73, 124.72, 137.61, 148.88. MS (gc/ms) *m*/*z* (%): 314 (M^+, 8.4), 202 (100), 122 (41.4). HRMS: *m*/*z* calculated for $C_{16}H_{28}O_4P$ (MH^+) 315.1720. Found 315.0501.

*5.1.1.7. Di-n-butyl 3, 4, 5-trimethylphenyl phosphate (**4c**).* Following the general procedure described above and using 3, 4, 5-trimethylphenol, **4c** was obtained as a light yellow oil: 28% yield. ^{1}H NMR (300 MHz, $CDCl_3$) δ 0.92 (t, J = 7.4 Hz, 6H, ($OCH_2CH_2CH_2CH_3)_2$), 1.34–1.47 (m, 4H, ($OCH_2CH_2CH_2CH_3)_2$), 1.62–1.72 (m, 4H, ($OCH_2CH_2CH_2CH_3)_2$), 2.11 (s, 3H Ph-CH_3), 2.25 (s, 6H, Ph-($CH_3)_2$), 4.09–4.16 (m, 4H, ($OCH_2CH_2CH_2CH_3)_2$), 6.86 (s, 2H, Ar-*H*); ^{13}C NMR (100 MHz, $CDCl_3$) δ 13.72, 15.00, 18.75, 20.85, 32.34, 68.24, 118.81, 131.83, 137.96, 147.95. MS (GC/MS) *m*/*z* (%): 328 (M^+, 25), 216 (100), 91 (63). HRMS: *m*/*z* calculated for $C_{17}H_{30}O_4P$ (MH^+) 329.1876. Found 329.1846.

*5.1.1.8. Di-n-butyl 1-naphthyl phosphate (**5a**).* Following the general procedure described above and using 1-naphthol, **5a** was obtained as an orange oil: 48% yield. ^{1}H NMR (400 MHz, $CDCl_3$) δ 0.87 (t, J = 7.4 Hz, 6H, ($OCH_2CH_2CH_2CH_3)_2$), 1.31–1.41 (m, 4H, ($OCH_2CH_2CH_2CH_3)_2$), 1.61–1.68 (m, 4H, ($OCH_2CH_2CH_2CH_3)_2$), 4.13–4.24 (m, 4H, ($OCH_2CH_2CH_2CH_3)_2$), 7.38–7.19 (m, 7H, Naph-*H*); ^{13}C NMR (100 MHz, $CDCl_3$) δ 11.65, 16.78, 30.46, 66.62, 113.09,119.83, 122.96, 123.67, 124.60, 124.67, 124.77, 125.92, 132.96, 144.96. MS (gc/ms) *m*/*z* (%): 336 (M^+, 100), 224 (93.6), 144 (48.9). HRMS: *m*/*z* calculated for $C_{18}H_{26}O_4P$ (MH^+) 337.1563. Found 337.1552.

*5.1.1.9. Di-n-butyl 2-naphthyl phosphate (**5b**).* Following the general procedure described above and using 2-naphthol, **5b** was obtained as a dark yellow oil: 36.8% yield. ^{1}H NMR (300 MHz, $CDCl_3$) δ 0.93 (t, J = 7.4 Hz, 6H, ($OCH_2CH_2CH_2CH_3)_2$), 1.36–1.48 (m, 4H, ($OCH_2CH_2CH_2CH_3)_2$), 1.66–1.75 (m, 4H, ($OCH_2CH_2CH_2CH_3)_2$), 4.16–4.25 (m, 4H, ($OCH_2CH_2CH_2CH_3)_2$), 7.37–7.85 (m, 7H, Naph-*H*); ^{13}C NMR (75 MHz, $CDCl_3$) δ 13.55, 18.64, 32.29, 68.42, 116.36, 120.03, 125.44, 126.70 127.53, 127.71, 129.82, 130.90, 133.90, 148.39. MS (gc/ms) *m*/*z* (%): 336 (M^+, 46.6), 224 (100), 115 (76.9). HRMS: *m*/*z* calculated for $C_{18}H_{26}O_4P$ (MH^+) 337.1563. Found 337.1548.

*5.1.1.10. Benzyl di-n-butyl phosphate (**6a**).* Following the general procedure described above and using benzyl alcohol, **6a** was obtained as a light yellow oil: 33% yield. ^{1}H NMR (300 MHz, $CDCl_3$) δ 0.91 (t, J = 7.2 Hz, 6H, ($OCH_2CH_2CH_2CH_3)_2$), 1.32–1.44 (m, 4H, ($OCH_2CH_2CH_2CH_3)_2$), 1.58–1.67 (m, 4H, ($OCH_2CH_2CH_2CH_3)_2$), 3.98–4.06 (m, 4H, ($OCH_2CH_2CH_2CH_3)_2$), 5.07 (d, J = 8.1 Hz, 2H, (OCH_2-Ph), 7.35–7.42 (m, 5H, Ph-*H*); ^{13}C NMR (75 MHz, $CDCl_3$) δ

13.57, 18.64, 32.28, 67.58, 69.05, 127.86, 128.55, 136.18, 140.52. MS (gc/ms) *m*/*z* (%): 300 (M^+, 25.4), 188 (100), 91 (77.5). HRMS: *m*/*z* calculated for $C_{15}H_{26}O_4P$ (MH^+) 301.1563. Found 301.1551.

*5.1.1.11. Di-n-butyl o-methylbenzyl phosphate (**6b**).* Following the general procedure described above and using *o*-methylbenzyl alcohol, **6b** was obtained as a colorless oil: 42% yield. ^{1}H NMR (300 MHz, $CDCl_3$) δ 0.92 (t, J = 7.4 Hz, 6H, $(OCH_2CH_2CH_2CH_3)_2$), 1.32–1.44 (m, 4H, $(OCH_2CH_2CH_2CH_3)_2$), 1.58–1.68 (m, 4H, $(OCH_2CH_2CH_2CH_3)_2$), 2.38 (s, 3H, Ph-CH_3), 3.97–4.06 (m, 4H, $(OCH_2CH_2CH_2CH_3)_2$), 5.09 (d, J = 7.5 Hz, 2H, OCH_2-Ar), 7.18–7.40 (m, 4H, Ar-*H*); ^{13}C NMR (75 MHz, $CDCl_3$) δ 11.57, 18.65, 32.20, 67.46, 126.02, 128.70, 128.86134.08, 136.76. MS (gc/ms) *m*/*z* (%): 314 (M^+, 4.0), 201 (27.2), 105 (100). HRMS: *m*/*z* calculated for $C_{16}H_{28}O_4P$ (MH^+) 315.1720. Found 315.1724.

*5.1.1.12. Di-n-butyl m-methylbenzyl phosphate (**6c**).* Following the general procedure described above and using *m*-methylbenzyl alcohol, **6c** was obtained as a light yellow oil: 40% yield. ^{1}H NMR (400 MHz, $CDCl_3$) δ 0.90 (t, J = 7.4 Hz, 6H, $(OCH_2CH_2CH_2CH_3)_2$), 1.32–1.42 (m, 4H, $(OCH_2CH_2CH_2CH_3)_2$), 1.58–1.65 (m, 4H, $(OCH_2CH_2CH_2CH_3)_2$), 2.35 (s, 3H, Ph-CH_3), 3.95–4.04 (m, 4H, $(OCH_2CH_2CH_2CH_3)_2$), 5.02 (d, J = 8.0 Hz, 2H, OCH_2-Ar), 7.15–7.27 (m, 4H, Ar-*H*); ^{13}C NMR(100 MHz, $CDCl_3$) δ 11.72, 16.83, 19.50, 30.47, 65.71, 67.27, 123.09, 126.71, 126.78, 127.32, 134.31, 136.41. MS (gc/ms) *m*/*z* (%): 314 (M^+, 7.9), 202 (60.5), 105 (100). HRMS: *m*/*z* calculated for $C_{16}H_{28}O_4P$ (MH^+) 315.1720. Found 315.1720.

*5.1.1.13. Di-n-butyl p-methylbenzyl phosphate (**6d**).* Following the general procedure described above and using *p*-methylbenzyl alcohol, **6d** was obtained as a red-orange oil: 36% yield. ^{1}H NMR (300 MHz, $CDCl_3$) δ 0.92 (t, J = 7.4 Hz, 6H, $(OCH_2CH_2CH_2CH_3)_2$), 1.32–1.44 (m, 4H, $(OCH_2CH_2CH_2CH_3)_2$), 1.58–1.67 (m, 4H, $(OCH_2CH_2CH_2CH_3)_2$), 2.36 (s, 3H, Ph-CH_3), 3.97–4.05 (m, 4H, $(OCH_2CH_2CH_2CH_3)_2$), 5.03 (d, J = 8.4 Hz, 2H, OCH_2-Ar), 7.17–7.30 (m, 4H, Ar-*H*); ^{13}C NMR(100 MHz, $CDCl_3$) δ 13.58, 18.64, 21.21, 32.29, 67.44, 69.05, 128.06, 129.21, 133.19, 138.32. MS (gc/ms) *m*/*z* (%): 314 (M^+, 10.4), 202 (100), 121 (79.7). HRMS: *m*/*z* calculated for $C_{16}H_{28}O_4P$ (MH^+) 315.1720. Found 315.1732.

*5.1.1.14. Di-n-butyl 2-phenylethyl phosphate (**7**).* Following the general procedure described above and using 2-phenylethanol, **7** was obtained as a light yellow oil: 45% yield. ^{1}H NMR (400 MHz, $CDCl_3$) δ 0.90 (t, J = 7.4 Hz, 6H, $(OCH_2CH_2CH_2CH_3)_2$), 1.31–1.41 (m, 4H, $(OCH_2CH_2CH_2CH_3)_2$), 1.56–1.63 (m, 4H, $(OCH_2CH_2CH_2CH_3)_2$), 2.98 (t, J = 7.0 Hz, 2H, OCH_2CH_2-Ph), 3.89–3.99 (m, 4H, $(OCH_2CH_2CH_2CH_3)_2$), 4.19–4.24 (q, J = 7.1 Hz, 2H, $(OCH_2CH_2$-Ph), 7.20–7.31 (m, 5H, Ph-*H*); ^{13}C NMR(100 MHz, $CDCl_3$) 13.56, 18.64, 32.18, 50.45, 67.59, 69.05, 127.86, 122.44, 128.55, 136.19. MS (gc/ms) *m*/*z* (%): 314 (M^+, 0.1), 105 (100), 77 (26.5).

*5.1.1.15. Diethyl 3,5-dimethylphenyl phosphate (**8**).* Following the general procedure described above and using diethyl chlorophosphate (**10**) and 3, 5-dimethylphenol, **8** was obtained as a yellow oil: 39% yield. ^{1}H NMR (400 MHz, $CDCl_3$) δ 1.37 (t, J = 7.0 Hz, 6H, $(OCH_2CH_3)_2$), 2.31 (s, 6H, Ph-$(CH_3)_2$), 4.18–4.26 (m, 4H, $(OCH_2CH_3)_2$), 6.81 (s, 1H, Ar-*H*), 6.84 (s, 2H, Ar-*H*); ^{13}C NMR (100 MHz, $CDCl_3$) δ 16.23, 21.43, 64.60, 117.61, 126.80, 139.67, 150.59. MS (GC/MS) *m*/*z* (%): 258.1 (M^+, 29.6), 132.1 (100), 122.1 (90.8). HRMS: *m*/*z* calculated for $C_{12}H_{20}O_4P$ (MH^+) 259.1094. Found 259.1127.

*5.1.1.16. Diethyl 2-naphthyl phosphate (**9**).* Following the general procedure described above and using diethyl chlorophosphate (**10**) and 2-naphthol, **9** was obtained as a dark yellow oil: 56% yield. ^{1}H NMR (400 MHz, $CDCl_3$) δ 1.37 (t, J = 7.0 Hz, 6H, $(OCHCH_3)_2$), 4.21–4.30 (m, 4H, $(OCH_2CH_3)_2$), 7.26–7.84 (m, 7H, Naph-*H*); ^{13}C NMR (100 MHz, $CDCl_3$) δ 16.57, 65.13, 116.76, 120.49, 125.90, 127.14 127.97, 128.14, 130.29, 131.26, 134.25, 148.76. MS (GC/MS) *m*/*z* (%): 280.0 (M^+, 32.9), 144.0 (89.8), 115.0 (100). HRMS: *m*/*z* calculated for $C_{14}H_{18}O_4P$ (MH^+) 281.0937. Found 281.0952.

5.2. Inhibition measurements

Butyrylcholinesterase from equine serum (Sigma-Aldrich catalog number: C7512) and acetylcholinesterase from *Electrophorus electricus* (Sigma-Aldrich catalog number: C3389) were purchased from Sigma-Aldrich. Inhibition measurements were performed based on the method of Ellman as described in Law et al. with minor modifications.[16] Reactions were conducted at 25 °C in 100 mM sodium phosphate, pH 7.5, 1 mM $MgCl_2$, 0.2 mM 5,5′-dithiobis-(2-nitrobenzoic acid) (DTNB), 1.2 μg/μl BSA, 100 μM butyrylthiocholine, and 2% methanol as a cosolvent. A reaction without inhibitor and 2% methanol was run as a no inhibitor control and a reaction without enzyme was run to determine the background absorbance change over the time of the reaction. Reactions were initiated by adding enzyme (10 nM final concentration) and initial rates were determined by monitoring continuously at 412 nm in a PerkinElmer Lambda 25 spectrophotometer. A molar absorptivity of 14,150 M^{-1} cm^{-1} was used. Values of K_I were obtained from the dependence of the observed rate constant on the concentration of inhibiting phosphate ligand (typically twelve concentrations). At least three determinations were averaged for each inhibitor.

Substrate rescue experiments were performed using the conditions described above except that the substrate concentration was varied and reactions were initiated by adding substrate. Activity was first determined without inhibitor and 2% methanol using substrate concentrations of 150 μM and 25 mM. Reactions were then run at 150 μM and 25 mM substrate in the presence of inhibitor concentrations near the calculated K_I value for each compound. For each reaction the enzyme and inhibitor were incubated for one minute prior to initiation of the reaction by substrate addition. Relative activity was calculated by dividing the initial rate for reaction with 25 mM substrate in the presence of the inhibitor by the reaction without inhibitor. The reactions with 150 μM substrate were run as a control to determine that inhibition was observed for each compound under the conditions for the experiment.

Relative activity measurements for BChE and AChE were conducted as described above except that for AChE reactions 100 μM acetylthiocholine was used as the substrate and reactions were initiated by the addition of acetylcholinesterase (10 nM final concentration). Reactions were performed with 2% methanol (no inhibitor) and 500 μM inhibitor (final concentration) in 2% methanol. Relative activity was determined by dividing the initial rate for reaction in the presence of each compound by control reaction. At least three determinations using independently prepared solutions of the inhibitors were measured and averaged.

Assays using α-chymotrypsin were conducted essentially as previously described.[20] α-Chymotrypsin was purchased from MP Biomedicals (Catalog No. 02152272). Reactions were conducted at 25 °C in 38 mM Tris-HCl, pH 7.8, 53 mM $CaCl_2$, 0.03 mM HCl, 32% methanol, and 0.55 mM *N*-benzoyl-l-tyrosine ethyl ester (Alfa Aesar). A solution of chymotrypsin containing 5 units per mL in ice-cold 1 mM HCl was prepared immediately before use. Prior studies reported 30% methanol as the organic cosolvent concentration. Reactions herein contained 32% methanol, as 30% methanol was used to parallel literature conditions for substrate solubility and an additional 2% methanol cosolvent was from addition of the inhibitor in a methanol solution. Reactions were performed without inhibitor and with 500 μM inhibitor (final concentration of 32% methanol in all reactions). The reactions were initiated by addition of enzyme and initial rates were determined by monitor-

ing continuously at 256 nm. A reaction without enzyme was run to determine the background absorbance change. Relative activity was calculated by dividing the initial rate for reaction in the presence of each compound by control reaction. At least two determinations using independently prepared solutions of the inhibitors were measured and averaged.

5.3. Molecular modeling studies

A model of human BChE was prepared by removing all water, ions, and ligands from the crystal structure (PDB ID: 1P0I), inserting missing atoms and sidechains (none of which were near or part of the enzyme active site gorge), and performing geometry optimization on these regions using Accelrys Discovery Studio.[21] The resulting structure was then energy minimized, including sidechain rotamer relaxation, using the SwissPDB software.[22] Computational docking of flexible dialkyl phenyl phosphate derivatives with this energy minimized BChE structure was then carried out using ICM-Pro version 3.7-2b.[23] ICM PocketFinder[24] readily and consistently identifies the active site receptor region of BChE, facilitating automation of massive docking trials. For each inhibitor studied, 10,000–20,000 such trials were undertaken using the default thoroughness value of 1.0, with the best-scoring structure from each trial saved for structural analysis.

Acknowledgments

The authors thank Silvia A. Cervantes, Minh N. H. Nguyen, Phuong A. T. Nguyen and Jocelyn Ochoa for assistance in synthesis of the analogs; Eric Armas for assistance with inhibition experiments; and Ji Won Lee for assistance with computational modeling. The authors are also grateful to the NSF for the purchase of the high-field NMR spectrometer (NSF MRI CHE-1337559). This work was supported in part by the Hispanic Serving Institutions Science, Technology, Engineering, and Math (HSI-STEM) program at California State University Long Beach funded by the Department of Education (J.P.S., J.G., and E.A.) as well as by the NIH-NIGMS Bridges to the Baccalaureate Grant 5R25GM050089 (J.O.). S.M. and W.A. would like to acknowledge support in the form of a Kenneth L. Marsi Scholarship and a Margaret Heeb Summer Research Scholarship, respectively.

A. Supplementary data

Supplementary data associated with this article can be found, in the online version, at http://dx.doi.org/10.1016/j.bmc.2017.04.002.

References

1. Farlow MR, Cummings JL. *Am J Med*. 2007;120:388–397.
2. Perry EK, Perry RH, Blessed G, Tomlinson BE. *Neuropath Appl Neuro*. 1978;4:273–277.
3. Bartus RT, Dean RL, Beer B, Lippa AS. *Science*. 1982;217:408–414.
4. Grossberg GT. *Curr Ther Res*. 2003;64:216–235.
5. Giacobini E. *Pharmacol Res*. 2004;50:433–440.
6. Greig NH, Utsuki T, Yu Q-S, et al. *Curr Med Res Opin*. 2001;17:159–165.
7. Greig NH, Utsuki T, Ingram DK, et al. *Proc Natl Acad Sci USA*. 2005;102:17213–17218.
8. Furukawa-Hibi Y, Alkam T, Nitta A, et al. *Behav Brain Res*. 2011;225:222–229.
9. Moretto A. *Toxicol Lett*. 1998;102–103:509–513.
10. Casida JE, Quistad GB. *Chem Biol Interact*. 2005;157–158:277–283.
11. Masson P, Lockridge O. *Arch Biochem Biophys*. 2010;494:107–120.
12. Makhaeva GF, Aksinenko AY, Sokolov VB, Serebryakova OG, Richardson RJ. *Bioorg Med Chem Lett*. 2009;19:5528–5530.
13. Shenouda J, Green P, Sultatos L. *Toxicol Appl Pharm*. 2009;241:135–142.
14. Kaboudin B, Emadi S, Hadizadeh A. *Bioorg Chem*. 2009;37:101–105.
15. Kratky M, Stepankova S, Vorcakova K, Vinsova J. *Bioorg Chem*. 2015;58:48–52.
16. Law K-S, Acey RA, Smith CR, et al. *Biochem Biophys Res Commun*. 2007;355:371–378.
17. Jann MW, Cyrus PA, Eisner LS, Margolin DL, Griffin T, Gulanski B. *Clin Ther*. 1999;21:88–102.
18. Levy D, Ashani D. *Biochem Pharmacol*. 1986;35:1079–1085.
19. Hosea NA, Berman HA, Taylor P. *Biochemistry*. 1995;34:11528–11536.
20. Chymotrypsin. In: Wirnt R, Bergmeyer HU, eds. *Methods of Enzymatic Analysis*. NY, New York: Academic Press; 1974:1009–1012.
21. http://accelrys.com/products/discovery-studio/.
22. Guex N, Peitsch MC. *Electrophoresis*. 1997;18:2714–2723.
23. Abagyan R, Totrov M, Kuznetsov D. *J Comput Chem*. 1994;15:488–506.
24. An J, Totrov M, Abagyan R. *Mol Cell Proteomics*. 2005;4:752–761.